Письма в ЭЧАЯ. А. 2012. Т. 9, № 9–10. С. 42–53

MEASURING OF MASS AND SPIN OF DARK MATTER PARTICLES AT ILC

I. F. Ginzburg [1]

Sobolev Institute of Mathematics, SB RAS,
and Novosibirsk State University, Novosibirsk, Russia

In many models, stability of dark matter particles D (with mass M_D) is ensured by a new conserved quantum number which we call the D-parity. We consider models which also contain charged D-odd particle $D^{\pm}$ (with mass $M_{\pm}$). We study the process $e^+e^- \to D^+D^-$ followed by decay of $D^{\pm}$ to D and gauge bosons W (either on-shell or off-shell). Measuring the end points of the energy distribution of W's would determine M_D and $M_{\pm}$. However, the hadron mode of W decay would lead to low precision in this measurement, while the information from the lepton mode looks incomplete.

We show that it is sufficient to measure the energy distribution of a single lepton (for definiteness μ) in the process $e^+e^- \to \mu + 2\,jets + large\ missing\ E_T$. The well identified singularities in this distribution allow for determination of M_D and $M_{\pm}$ with a high precision. After that, measuring the corresponding cross section will allow one to determine the spin of D particles.

Во многих моделях стабильность частиц темной материи D (с массой M_D) обеспечивается сохранением нового квантового числа, которое мы называем здесь D-четностью. Рассматриваются модели, которые содержат еще и заряженные D-нечетные частицы $D^{\pm}$ (с массой $M_{\pm}$). Мы изучаем процесс $e^+e^- \to D^+D^-$ с последующим распадом на D и W (реальный или виртуальный). Измерение концевых точек энергетического распределения W позволило бы определить массы M_D и $M_{\pm}$. Однако использование адронной моды распада W может претендовать только на низкую точность в этих массах, а информация из лептонных мод кажется недостаточной.

Мы показываем, что достаточно измерить энергетическое распределение единичного мюона в процессе $e^+e^- \to \mu + 2\ jets +$ *большая потерянная поперечная энергия*. Хорошо выделяемые особые точки этого распределения позволяют определить M_D и $M_{\pm}$ с хорошей точностью. После этого измерение соответствующего полного сечения позволяет определить спин D-частиц.

PACS: 14.80.-j; 14.80.Ly; 12.60.-i; 12.60.Jv

INTRODUCTION

In many models Dark Matter (DM) consists of DM particles (DMP) D similar to the SM particles. In these models DMP is stable due to conservation of a new discrete quantum number denoted below as the D-parity. This is a multiplicative quantum number which can be $+1$ (D-even particles) or -1 (D-odd particles). All particles known so far are D-even, while the DM particle is assumed to be D-odd. We consider models in which in addition to the neutral D-odd particle D with mass M_D there is a charged D-odd particle $D^{\pm}$ with mass $M_{\pm} > M_D$. We also allow one additional neutral D-odd particle D^A with mass $M_A > M_D$.

[1] E-mail: ginzburg@math.nsc.ru

These D particles have identical spin [1] $s_D = 0$ or $1/2$. In these models the D particles interact with the SM particles only via the covariant derivative in the kinetic term of the Lagrangian, that is via gauge interactions with the standard electroweak gauge couplings g and g' (in some cases, up to weights given by mixing angles of the model): $D^+D^-\gamma$, D^+D^-Z, D^+DW^-, D^ADZ, $D^\pm D^A W^\mp$. In the numerical calculations and estimates we assume that the masses of D particles differ from each other by more than 3–5 GeV.

Discovery of such candidates for DMP and other D-odd particles and measuring their properties is an important problem for the collider physics. At the LHC it is difficult to expect high precision in the DMP mass measurement and to propose a robust procedure for finding its spin. Linear e^+e^- colliders, ILC or CLIC, would open this window for a wide class of models. Two main processes for production of D particles at ILC/CLIC are crucial for their discovery and measurement of their masses and spin,

$$e^+e^- \to D^+D^-, \tag{1}$$

$$e^+e^- \to DD^A. \tag{2}$$

Once produced, $D^\pm$ and D^A quickly decay into $DW^\pm$ and DZ with either on-shell or off-shell W or Z. The off-shell W^* or Z^* is understood as dileptonic or diquark (dijet) state with quantum numbers of W or Z and the effective mass M^*. If $M_\pm > M_A$, the cascade decay $D^+ \to W^+D^A \to W^+ZD$ is possible as well. If $M_\pm < M_A$, the cascade decay $D^A \to W^\pm D^\mp \to W^+W^-D$ is possible.

Non-observation of process (1) at LEP II implies that $M_\pm > 80$ GeV [3]. The DMP mass is limited by its stability during life of Universe [4, 5].

The cross sections of processes (1), (2) are of the same order as the reference quantity $\sigma_0 \equiv \sigma(e^+e^- \to \gamma \to \mu^+\mu^-) = 4\pi\alpha^2/3s$. Note that the total cross section of the e^+e^- annihilation at the ILC (including processes $e^+e^- \to ZZ$ and $e^+e^- \to WW$) is $\sim 10\sigma_0$.

The end points in the energy distributions of dijets or dileptons, representing W or Z in the main decay, can be used for finding masses $M_\pm$ and M_D or M_A and M_D, respectively, see, e.g., [5]. Unfortunately, due to well-known uncertainties in the measurement of individual jet energies, this method will have low accuracy for dijet ($q\bar{q}$) modes. With leptons, one can count on higher precision in energy distribution. It can be used for measuring M_D and M_A, if these masses are in the attainability domain for reaction (2). However, the study of this process cannot be used for measuring spin s_D.

The process (1) with decay $D^\pm \to DW^\pm$ gives only one lepton from the pair, representing the W, and the method based on end points cannot be applied directly. We found that the energy distribution of single muons in the final state ($dijet\ + \mu\,(e) +\ nothing$) has enough singular points for determining through them the masses $M_\pm$ and M_D. After that, one can determine the spin s_D.

[1] The well-known example of such a model with $s_D = 1/2$ is MSSM. Here D is the lightest neutralino, D^A is another neutralino and $D^\pm$ is the lightest chargino [1]; D-parity being another name for the R-parity.

In the inert doublet model (IDM) [2] $s_D = 0$. In addition to the Higgs doublet ϕ_S, the same as in SM, the IDM contains another scalar doublet ϕ_D with zero vacuum expectation value and no coupling to fermions. The components of ϕ_D form massive D-odd particles: a charged $D^\pm$ and two neutrals D^A and D, the latter being DMP.

1. THE PROCESS $e^+e^- \to D^+D^-$

1.1. Basics. To set kinematical notation, we introduce the energies, γ factors and velocities of $D^\pm$ in c.m.s. for e^+e^- as

$$E_\pm = E = \frac{\sqrt{s}}{2}, \quad \gamma_+ = \frac{E}{M_+}, \quad \beta_+ = \sqrt{1 - \frac{M_+^2}{E^2}}. \tag{3}$$

The cross section of this process is a significant part of the total e^+e^- annihilation cross section at ILC (see Table 1 and Fig. 1). Main part of this cross section is given by model-independent QED contribution of photon exchange; the model-dependent contribution of Z exchange at $\sqrt{s} > 200$ GeV contributes less than 30% to the total cross section. Neglecting small quantity $1/4 - \sin^2\theta_W$, we have (here Z exchange contribution is calculated for the weak isodoublet scalar or fermion)

$$\sigma(e^+e^- \to D^+D^-) = \sigma_0\beta_+ \begin{cases} \left[\dfrac{3-\beta_+^2}{2} + r_Z d_Z \beta_+^2\right] & \left(s_D = \dfrac{1}{2}\right), \\ \dfrac{\beta_+^2}{4}\left[1 + 4 r_Z d_Z \cos^2(2\theta_W)\right] & (s_D = 0), \end{cases} \tag{4}$$

$$r_Z = (2\sin(2\theta_W))^{-4} = 0.124, \quad d_Z = \left(1 - \frac{M_Z^2}{s}\right)^{-2}.$$

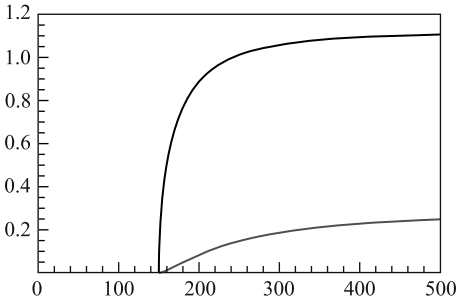

Fig. 1. The $\sigma(e^+e^- \to D^+D^-)/\sigma_0$ dependence on E, $M_\pm = 150$ GeV, upper curve — $s_D = 1/2$, lower curve — $s_D = 0$

Table 1

E, GeV	M_+, GeV	$E^W_{\rm up}$	E^W_d	s_D	σ/σ_0
100	80	47	20.1	0	0.066
				1/2	0.84
250	80	137	30.8	0	0.245
				1/2	1.107
250	150	195.4	98.6	0	0.169
				1/2	1.02
250	200	193.6	81.2	0	0.062
				1/2	0.82

1.2. The Case without D^A or at $M_A > M_\pm > M_D$. Observable Final States. Signature. The main decay channel for $D^\pm$ is $D^\pm \to DW^\pm$ and the observable process is

$$e^+e^- \to D^+D^- \to DDW^+W^-. \tag{5}$$

The final state observed in the detector contains only decay products of both W's and nothing else. In contrast to direct production of W^+W^- pair, this final state is also characterized by a large missing transverse energy $\not{E}_T$ (which to a good approximation is equal to minus the total transverse momentum of detected particles). This means that a large transverse momentum is carried away by the undetected neutrinos and also by the neutral and stable D particles.

• At $M_\pm - M_D > M_W$ we deal with production of real W with the well-known decay channels and branching ratios [5]. The fraction of events with two dijets from hadronic decays for both W's is $0.676^2 \approx 0.45$. The fraction of events with one dijet from $q\bar{q}$ decay of $W^\mp$ plus $\ell = \mu,\ e$ from lepton decay of $W^\pm$ is $2 \cdot 0.676 \cdot 2 \cdot (1 + 0.17) \cdot 0.108 \approx 0.33$ (here 0.17 is a fraction of μ or e from the decay of τ).

• If $M_\pm - M_D < M_W$, we deal with a decay to an off-shell W^*, whose effective mass is $M^* \leqslant M_+ - M_D$. At $M^* > 4$ GeV the decay modes and branching ratios for W^* decay are practically the same as for the on-shell W. At lower M^* the $c\bar{s}$ contribution decreases, and the corresponding BRs are naturally modified. The considered process has a clean signature:

Two dijets or one dijet plus e or μ with large $\not{E}_T +\ nothing$ with the total energy for each dijet or lepton lower than E. The effective mass of each dijet is $\leqslant M_W$. The missing mass of particles escaping observation is large. Typically these dijets (or a dijet and a lepton) move in the opposite hemispheres.	(6)

All these events must be considered when determining the total cross section. The fraction of these events with the final state ($dijet\ + \mu(e) +\ nothing$) must be considered when determining masses.

1.3. W **Energy Distribution**

• If $M_+ - M_D > M_W$, the effective mass of the $q\bar{q}$ or $\ell\nu$ pair is M_W. In the rest frame of $D^\pm$ we deal with a 2-particle decay $D^\pm \to DW^\pm$ with energy and momentum of W:

$$E_W^r = \frac{M_+^2 + M_W^2 - M_D^2}{2M_+}, \quad p_W^r = \frac{\Delta(M_+^2, M_W^2, M_D^2)}{2M_+},$$
$$\Delta(s,\, s_1,\, s_2) = \sqrt{s^2 + s_1^2 + s_2^2 - 2ss_1 - 2ss_2 - 2s_1s_2}. \tag{7}$$

Denoting by θ the W^+ escape angle in the D^+ rest frame with respect to the direction of D^+ motion in the lab frame and using $c \equiv \cos\theta$, we have the energy of W^+ in the lab frame $E_W^L = \gamma_+(E_W^r + c\beta_+ p_W^r)$. Therefore, the energy of $\ell\nu$ pairs or dijets from W decay lie within the interval [5] (see Table 1 for numerical examples)

$$E > E_W^{L,\mathrm{up}} = \gamma_+(E_W^r + \beta_+ p_W^r) \geqslant E_W^L \geqslant E_W^{L,d} = \gamma_+(E_W^r - \beta_+ p_W^r). \tag{8}$$

This distribution is uniform in energy, $d\sigma/dE_W^L = \mathrm{const}$. At $s_D = 0$ it is evident since $D_\pm$ decay in the rest frame is isotropic. At $s_D = 1/2$ this uniformity appears after $D_\pm$ production angle averaging.

• If $M_+ - M_D < M_W$, we deal with the decay $D^\pm \to DW^{*\pm}$. At each value M^* of the effective mass of W^*, the energy and momentum of W^* in the $D^\pm$ rest frame are given by Eq. (7) and in the lab frame by Eq. (8) with $M_W \to M^*$. In particular, at the boundaries of the M^* interval, the end point values of energy distribution of dijets are

$$E_W^{L,\mathrm{up};\,d}(M^* = 0) = \gamma_+(1 \pm \beta_+)\frac{M_\pm^2 - M_D^2}{2M_\pm},$$
$$E_W^{L,\mathrm{up}}(M^* = M_\pm - M_D) = E_W^{L,d}(M^* = M_\pm - M_D) = \gamma_+(M_\pm - M_D). \tag{9}$$

The effective mass M^*-distribution of the $\ell\nu$ pairs or dijets ($q\bar{q}$) is given by the spin-dependent factor $R_{s_D} dM^*$ (we neglect small $1/4 - \sin^2\theta_W$):

$$R_0 = \frac{p^{*3}\, M^*}{(M_W^2 - M^{*2})^2},$$
$$R_{1/2} = \left[\frac{2(M_\pm^2 + M_D^2 - M^{*2})}{(M_W^2 - M^{*2})^2} - \frac{(M_\pm^2 + M_D^2)M^{*2} - (M_\pm^2 - M_D^2)^2}{(M_W^2 - M^{*2})^2 M_W^2}\right] p^*\, M^*. \tag{10}$$

1.4. The Lepton Energy Distribution from the Cascade Decay $D^+ \to DW^+ \to D\ell^+\nu$ (for definiteness, $\ell = \mu$; muon mass neglected)

• If $M_+ - M_D > M_W$, the muon energy and momentum in the rest frame of W are $M_W/2$. The γ-factor and the velocity of W in the lab frame are $\gamma_{WL} = E_W^L/M_W$ and $\beta_{WL} \equiv \sqrt{1 - \gamma_{WL}^{-2}}$. Just as above, denoting by θ_1 the escape angle of μ relative to the direction of the W in the lab frame and $c_1 = \cos\theta_1$, we find that for given value E_W^L, the muon energy lies within the interval $E_{\mu+}^{WL} \geqslant E_\mu \geqslant E_{\mu-}^{WL}$, where

$$E_{\mu(\pm)}^{WL} = \frac{1}{2} E_W^L (1 \pm \beta_{WL}) = \frac{1}{2}\left(E_W^L \pm \sqrt{(E_W^L)^2 - M_W^2}\right).$$

As the energy E_W^L decreases, the interval shrinks too. For any fixed value of E_W^L, the muon energy distribution is uniform. Therefore, when taking into account all possible E_W^L, (8), we find the overall range of muon energies $\geqslant E_\mu \geqslant E_{\mu-}^L$, where

$$E_{\mu\pm}^L = \frac{1}{2}\left(E_W^{L,\mathrm{up}} \pm \sqrt{(E_W^{L,\mathrm{up}})^2 - M_W^2}\right). \tag{11}$$

The total density of states within this interval increases monotonically from outer limits up to the energies which correspond to $E_W^{L,d}$ (see Fig. 2)

$$E_{\mu(s\pm)} = \frac{1}{2}\left(E_W^{L,d} \pm \sqrt{(E_W^{L,d})^2 - M_W^2}\right). \tag{12}$$

• If $M_+ - M_D < M_W$, the $D^\pm$ decays to D and an off-shell W^* with an effective mass M^*. The calculations, similar to above, for each $M^* \leqslant M_+ - M_D$ with Eq. (9) taken into account, show that the muon energies lie within the interval, appearing at $M^* = 0$:

$$\left(E_{\mu(+)}^* = \gamma_+(1+\beta_+)\frac{M_+^2 - M_D^2}{2M_+}, \quad E_{\mu(-)}^* = 0\right). \tag{13}$$

Similarly to the previous discussion, increase of M^* leads to a downward shift of the upper bound of the interval, and the upward shift of its lower bound. Therefore, the density of states in muon energy increases monotonically with decreasing of energy from $E_{\mu(+)}^*$ up to the maximum at

$$E_{\mu s}^L = \gamma_+(1+\beta_+)(M_+ - M_D)/2. \tag{14}$$

This density is calculated by convolution of the kinematically defined distribution like Fig. 2 with the effective mass distribution (10). The result is shown in Fig. 3. Its important feature is a rather sharp peak at $E = E_{\mu s}^L$ for each value of spin s_D.

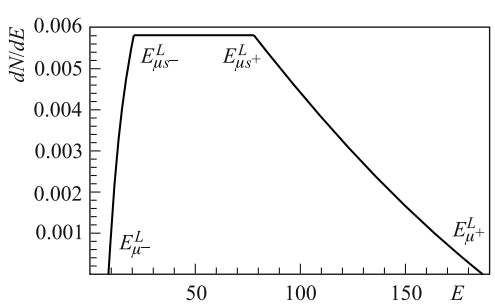

Fig. 2. The muon energy distribution at $E = 250$ GeV, $M_D = 50$ GeV, $M_\pm = 150$ GeV (on-shell W)

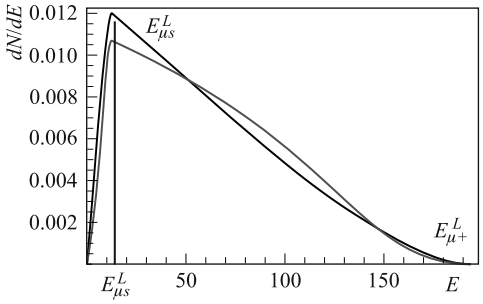

Fig. 3. The normalized muon energy distribution at $E = 250$ GeV, $M_D = 50$ GeV, $M_\pm = 120$ GeV (off-shell W). The upper and lower peaks are for $s_D = 0$ and $s_D = 1/2$, respectively

1.5. The Background

$BW1$. The process $e^+e^- \to W^+W^-$ gives in principle the same final state as our process (5). However, this process has many features that are not compatible with the signature (6) (see also Table 1). (A) Energy of each dijet equals E. (B) For the detected final state dijet+dijet, the observed $\not{E}_T$ will be low (ideally, zero). (C) For the detected final state dijet+lepton, the missing mass of the unobserved state will be low (ideally, zero). These differences allow for exclusion of the process $BW1$ with good confidence. Even those few events coming from the tails of the distributions that can pass the kinematical cuts will give muons uniformly distributed in the energy interval between $(E - \sqrt{E^2 - M_W^2})/2$ and $(E + \sqrt{E^2 - M_W^2})/2$, which is wider than the one described above. This small background can be easily eliminated from the observed energy distribution of muons.

$BW2$. In other SM processes where final states satisfying criterion (6) are produced, the large $\not{E}_T$ is carried away by additional neutrinos. The corresponding cross section is at least $g^2/4\pi$ or $g'^2/4\pi$ smaller than σ_0, where g and g' are electroweak coupling constants and $g^2/4\pi \sim g'^2/4\pi \sim \alpha$. Therefore, the cross sections of these background processes are about one order of magnitude smaller than the signal cross section.

$BW3$. The decay channel $W \to \tau\nu \to \mu\nu\nu\nu$ (BR $= 17\%$). The energy of muon produced in this cascade decay lies between 0 and $M_\tau/2$ in the τ rest frame. These muons change the estimated distributions by a small correction (17%, distributed over energy interval by a law $2(3 - 2\varepsilon)\varepsilon^2 d\varepsilon$, where ε is ratio of muon energy in the τ rest frame to $m_\tau/2$). This contribution is a smooth distribution with no cusps, and therefore it can be considered as small correction in numerical simulation.

$BW4$. The process $e^+e^- \to Z \to DD^A \to DD^\pm W^\mp \to DDW^+W^-$, at first glance, could represent a significant background to the phenomenon we consider. In reality, it is not so important due to several reasons. (A) Its cross section is lower than that of our process $e^+e^- \to D^+D^- \to DDW^+W^-$ by about one order of magnitude. This is because the DD^A production cross section is typically 3–5 times smaller than for the D^+D^- production even at $M_A \approx M_\pm$. Besides, BR$(D^A \to D^\pm W^\mp)$ is less than 1/2 due to the lower phase space as compared with the main decay $D^A \to DZ$. (B) In the process $BW4$ all recorded particles move in one hemisphere in contrast to the process (5), where they are back to back, (6). (C) In

the process $BW4$ the total energy of recorded particles is lower than the beam energy E, while in the process (5) the total energy is larger than E for most events.

1.6. The Case $M_\pm > M_A > M_D$. Additional Observable Final States. In this case one more decay chain is allowed, $D^\pm \to D^A W^\pm \to DZW^\pm$. The decay $D^\pm \to D^A W^\pm$ is described by the same equation as $D^\pm \to DW^\pm$. Its probability is lower than that of $D^\pm \to DW^\pm$ due to the smaller final phase space, i.e.,

$$\mathrm{BR}\,(D^+ \to D^A W^+) < 0.5. \tag{15}$$

In addition to the basic process (5), the list of final states now contains products of W or Z decays from the following cascade processes:

$$e^+e^- \to D^+D^- \to \begin{cases} D^A W^\pm DW^\mp \to DDW^+W^-Z, & \text{(b)} \\ D^A W^+ D^A W^- \to DDW^+W^-ZZ. & \text{(c)} \end{cases} \tag{16}$$

The signature of these final states is rather simple and is similar to (6):

3 or 4 dijets, or fewer dijets plus 1 to 5 leptons with large $\not{E}_T + \ nothing$. The missing mass of particles escaping observation is large. The observed cluster in two groups moving in the opposite hemispheres, each of them having the total energy less than E.

(17)

1.7. One More Impact to Muon Distribution. For a generic Z decay, the processes (16) will be distinguishable from process (5). However, Z bosons can decay invisibly, ($Z \to \nu\bar{\nu}$), with branching ratio $\mathrm{BR} = 20\%$. Therefore, the processes (16) with invisibly decaying Z's will look as (5). They contribute additional events to the final state with signature $dijet + \mu + \ nothing$, which will be used for measuring M_D and $M_\pm$. This effect should be taken into account only after observation of the more probable process with signature (17).

In accordance with (15), for each final state ($dijet + \mu + \ nothing$) the relative fraction of these «wrong» muons is less than 1/6. The energy distributions of leptons in these processes are described by the same equations as for the main process $e^+e^- \to DDW^+W^-$ with the natural change $M_D \to M_A$. Therefore, distributions shown in Figs. 2 and 3 will be modified by contributions of the same shape but which are narrower and lower. Either these contributions will be negligible or one can extract them from the data to verify the value M_D and to determine M_A.

2. THE PROCESS $e^+e^- \to DD^A$

If the process $e^+e^- \to DD^A$ is kinematically allowed, the location of the end points in the energy distribution of dileptons from the decay $D^A \to DZ$ will give masses M_D and M_A with a good accuracy. However, even if M_D and M_A are known, the cross section of (2) strongly depends on details of the model and cannot be used for comparison of models and determination of s_D.

2.1. Basics. The energies, γ factors and velocities of D^A and D in c.m.s. for e^+e^- are

$$\begin{gathered} E_A = \frac{s + M_A^2 - M_D^2}{4E} \equiv \varepsilon_A E, \quad E_D = \frac{s - M_A^2 + M_D^2}{4E} \equiv \varepsilon_D E, \\ p_A = p_D = \frac{\Delta(s, M_A^2, M_D^2)}{4E}, \quad \gamma_A = \frac{E_A}{M_A}, \quad \beta_A = \frac{p_A}{E_A}, \quad \varepsilon_A + \varepsilon_D = 2. \end{gathered} \tag{18}$$

The cross section of the reaction at $M_A \sim M_\pm$ is lower than (4), and is of the order of few percent of the total e^+e^- annihilation cross section at ILC. In the IDM (with spin $s_D = 0$) it is (cf. (4))

$$\sigma(e^+e^- \to DD^A) = \sigma_0 r_Z d_Z \beta_A \varepsilon_A \beta_A^2 \varepsilon_A^2. \tag{19}$$

For spin 1/2 (e.g., in MSSM) the result depends on the nature of the D particle (Dirac or Majorana fermion), on mixing angles, etc.

Table 2. **The cross section $\sigma(e^+e^- \to DD^A)$ in IDM and the end point energies at various beam energies and masses M_A for fixed $M_D = 50$ GeV. The end point energies for $M_A = 80$ GeV are presented for the case $M^* = 20$ GeV**

E, GeV	M_A, GeV	σ/σ_0	$E_{\rm up}$	E_d^W
100	80	0.082	53.73	20.01
250	80	0.117	139.4	31.2
250	150	0.0945	206.3	133.4
250	200	0.0735	236	93
250	300	0.031	247	112

2.2. Observable Final State. Signature. The main decay channel of D^A is DZ. In this channel, the observed final state contains decay products of the $Z + \ nothing$ and a large missing transverse energy $\not{E}_T$, which is carried away by the neutral and stable D particle.

• At $M_A - M_D > M_Z$ we deal with production of real Z with well-known decay channels and branching ratios [5]. If $M_A - M_D < M_Z$, the decay involves the off-shell Z, $D^A \to DZ^*$, whose decay modes and branching ratios are nearly the same as for on-shell Z. At $M^* \lesssim 10$ GeV the $b\bar{b}$ contribution disappears, and the corresponding BRs are naturally modified.

The signature of this process in the Z-decay modes which are suitable for its observation (76% from total cross section) is clear:

> An e^+e^- or $\mu^+\mu^-$ pair or a quark dijet with large $\not{E}_T + \ nothing$. The effective mass of this pair or a dijet is either M_Z or lower than M_Z with identical distribution over all modes; its total energy is lower than E. The missing mass of undetected particles is large. (20)

• At $M_A > M_\pm$, an additional decay channel is possible, $D^A \to D^\pm W^\mp$, producing the cascade reaction $e^+e^- \to Z \to DD^A \to DD^\pm W^\mp \to DDW^+W^-$. The BR for this cascade process, $\mathrm{BR}\,(AW) < 0.5$, since the smaller final phase space at the first stage of cascade. This process differs from the main process $e^+e^- \to DDZ$, which can be used to find M_D, M_A. Its role as source of background is discussed below.

2.3. The Z-Boson Energy Distribution

• If $M_A - M_D > M_Z$, the effective mass of a dilepton or dijet ($q\bar{q}$ pair) is M_Z. In the rest frame of D^A we deal with the 2-particle decay $D^A \to DZ$ with the energy and momentum of the Z boson (compare with (7)):

$$E_Z^r = \frac{M_A^2 + M_Z^2 - M_D^2}{2M_A}, \quad p_Z^r = \frac{\Delta(M_A^2, M_Z^2, M_D^2)}{2M_A}. \tag{21}$$

Just as for $W^{\pm}$, we find that energy of dilepton pairs or dijets from Z decay lies within the interval (see Table 2 for numerical examples)

$$E > E^Z_{\rm up} = \gamma_A(E^r_Z + \beta_A p^r_Z) \geqslant E^L_Z \geqslant E^Z_d = \gamma_A(E^r_Z - \beta_A p^r_Z). \tag{22}$$

This energy distribution is uniform.

• If $M_A - M_D < M_Z$, the decay $D^A \to DZ^*$ involves an off-shell Z, and the effective mass of dilepton or a dijet ($q\bar{q}$ pair) is $M^* < M_A - M_D$. At each value of M^* the energy and momentum of this dijet or dilepton in the D^A rest frame can be written in the form (21) with $M_Z \to M^*$, and the positions of the end points in the Z^* energy distribution in the lab frame are given by Eq. (22) with the same replacement $M_Z \to M^*$.

2.4. Background. *For All Decay Modes*. The Z boson decays with $\mathrm{BR} = 0.2$ to invisible final states. Such invisibly decaying Z's will be denoted as Z_n. At first glance, the process $e^+e^- \to ZZ_n$ can mimic $e^+e^- \to DDZ$. However, the lepton or quark pairs in these processes have the same energy E as the colliding electrons. Therefore, the criterion (20) excludes such events from the analysis.

The cross section $\sigma(e^+e^- \to ZZ_n) \sim 0.2 \cdot 3r_Z\sigma_0 \ln(s/M_Z^2)$ is of the same order as (19). Therefore, the variants of this process with off-shell Z, giving another effective mass of observed dijet or dilepton and respectively another value of their energy, have cross section lower than (19). Similar estimates are valid for $e^+e^- \to \mu^+\mu^- Z_n$, $e^+e^- \to q\bar{q}Z_n$, and similar processes.

In other SM processes where the final states satisfy criterion (20), large $\not{E}_T$ is carried away by additional neutrino(s). The magnitude of the corresponding cross section is at least $g^2/4\pi$ or $g'^2/4\pi$ less than σ_0. Therefore, the background processes have cross sections which are one order smaller than the signal cross section.

For Leptonic Modes: the following processes can give essential contribution to $\ell^+\ell^-$ spectra:

$BZ1$ process $e^+e^- \to DDZ \to DD\tau\bar{\tau} \to DD\ell_1\bar{\ell}_2\nu\bar{\nu}$,

$BZ2$ cascade $e^+e^- \to DD^A \to DDW^+W^- \to DD\ell_1\bar{\ell}_2\nu\bar{\nu}$ (at $M_A > M_\pm$),

$BZ3$ process $e^+e^- \to \ell_1\bar{\ell}_2\nu\bar{\nu}$,

$BZ4$ process $e^+e^- \to D^+D^- \to DDWW \to DD\ell_1\bar{\ell}_2\nu\bar{\nu}$.

In all these processes, the two charged leptons are produced independently. Therefore, e^+e^-, $\mu^+\mu^-$, $e^-\mu^+$ and $e^+\mu^-$ pairs are produced with identical probability and identical distributions. Hence, the combination

$$(e^+e^- + \mu^+\mu^-) - (e^-\mu^+ + e^+\mu^-) \tag{23}$$

eliminates contribution of these processes from the energy distributions of interest. This procedure does not spoil the accuracy of the analysis if the cross sections of these processes after suitable cuts are kept moderate.

Process $BZ1$: this property is evident.

Cascade $BZ2$: the relative contribution of leptons from this cascade to the total $\mu^+\mu^-$ production is estimated simply as $\mathrm{BR}^2(W \to \mu\nu) \cdot \mathrm{BR}_{AW}/\mathrm{BR}\,(Z \to \mu^+\mu^-) \lesssim 0.2$.

The cross section of the process $e^+e^- \to W^+W^-$ with decays $W^\pm \to \ell^\pm\nu$ to identical leptons ($BZ3$) is $\sim 0.1^2\sigma_0 \ln(s/M_W^2)$, which is rather high. For our purposes, it can be strongly reduced by applying cuts on the total energy and effective mass of dileptons (20). In this process each of the observed leptons has energy and momentum within the interval $(0; E)$

without strong correlation between directions of momenta. Therefore, the dilepton energies and effective masses are distributed within the interval $(0; 2E)$. At $M_A - M_D > M_Z$ the anticipated events from our $e^+e^- \to DD^A$ process are discriminated well since for these events the effective mass of dilepton is M_Z. In the general case the signature condition (20) requires cuts $E_{\ell\bar{\ell}} < E$, $M_{\ell\bar{\ell}} \leqslant M_Z$. They reduce the cross section of the process $BZ2$ roughly by a factor $< (M_Z^2/s)^2 \ln(s/M_Z^2)$, which brings it below the signal cross section. Therefore, the procedure (23) removes this background.

Process $BZ4$. The basic cross section of process (4) is much lower than that of $BZ3$. In this process leptons are mainly back to back (6). For our purposes, the relevant cross section is reduced by cuts on the effective mass $M_{\ell\bar{\ell}} \leqslant M_Z$ and the condition that both leptons move in one hemisphere.

3. ALGORITHM FOR MEASURING MASSES AND SPIN

We summarize our analysis in an algorithmic procedure, which can be applied in order to measure the masses and spin of D particles.

• The observation of candidates with signature (6), (17), (20) will be a clear signal of the dark matter particles candidates.

• The study of the energy distribution of the only lepton produced in the process $e^+e^- \to DDW^+W^- \to\ dijet + \mu + \nu + \not{E}_T +\ nothing$ can lead to measurement of the masses M_D and $M_\pm$ with a good accuracy. We can meet here two opportunities.

a) In one case, this energy distribution grows from the upper and lower boundary to the central part where it is constant in some interval $(E_{\mu(s-)}, E_{\mu(s+)})$. In this case $M_\pm - M_D > M_W$, masses M_D and $M_\pm$ can be calculated from the equations for singular points $E_{\mu(s\pm)}$, (12), and the upper end point $E_\mu^{L,\mathrm{up}}$, (11).

b) In the other case, the muon energy distribution grows from the upper and lower boundary (the latter being zero) to the central peak at energy, $E_{\mu s}^L$ (14). In this case $M_\pm - M_D < M_W$, masses M_D and $M_\pm$ can be calculated from equation for the singular point $E_{\mu s}^L$, (14), and the upper end point $E_{\mu(+)}^*$, (13).

• The cross section of the process $e^+e^- \to D^+D^-$ is obtained by summation over all processes with signature (6), (17) with taking into account the known BRs for the W decay. On the other hand, when masses $M_\pm$ are determined, the cross section of $e^+e^- \to D^+D^-$ is calculated easily for each value of spin s_D, (4). Note that for identical masses $\sigma(s_D = 1/2) > 4\sigma(s_D = 0)$. This strong sensitivity to s_D allows for determination of the spin of D particle even if the cross section is poorly known.

• If the process $e^+e^- \to DD^A \to DDZ$ is observable, about 10% of the detected events with signature (20) — the ones involving dileptons e^+e^- and $\mu^+\mu^-$ — provide opportunity to measure the masses M_D and M_A with a good accuracy. To perform it, one needs to measure *(a) the effective mass of each lepton pair* and *(b) the total energy distribution of lepton pairs at each value of this effective mass.* The end points of this energy distribution will give these masses if Eqs. (22) etc. are considered as equations for M_A, M_D (cf. [5]). Note that this process does not allow one to determine s_D via the total cross section because it is strongly model-dependent. The latter point repeats the results of [5] with some new details.

4. COMPARING DIFFERENT COLLIDERS

The e^+e^- colliders have a number of advantages in studying these problems.

1. The cross section of the process (1) represents a large fraction of the total e^+e^- annihilation cross section. It depends on $M_\pm$ and spin s_D only, with a very strong sensitivity to s_D. Its experimental signature is very clean: note the word «*nothing*» in (6), (17)). A small associated background is given by the photon–photon production in the collision of ISR and beamstrahlung photons and the two-photon production of systems X, $e^+e^- \to e^+e^-X$.

At a hadron collider, such as the LHC, the cross section of the D^+D^- production represents a much lower fraction of the total hadron cross section, and it is accompanied with high background. Therefore, even the observation of $q\bar{q} \to D^+D^-$ process would be a difficult problem.

2. The kinematics of e^+e^- collision is precisely known, up to ISR and beamstrahlung. It allows one to measure singular points of the energy distribution of a single lepton (μ or e) with a high accuracy. This opportunity is absent at the LHC. One can try to measure instead the transverse momentum distributions of single lepton. At its best, it would allow one to measure one quantity (for example, $p_\perp^{\max}$), which cannot give information about two masses M_D and $M_\pm$.

This work was supported in part by grants RFBR 11-02-00242-a, NSh-3810.2010.2, the Program of Dept. of Phys. Sc. RAS «Experimental and theoretical studies of fundamental interactions related to LHC» and the Polish Ministry of Science and Higher Education Grant No. N202 230337. I am thankful to A. E. Bondar, A. G. Grozin, I. P. Ivanov, D. Yu. Ivanov, D. I. Kazakov, J. Kalinowski, K. A. Kanishev and V. G. Serbo for discussions.

REFERENCES

1. *Hooper D.* TASI 2008 Lectures on Dark Matter. arXiv:0901.4090;

   Maniatis M. The Next-to-Minimal Supersymmetric Extension of the Standard Model Reviewed // Intern. J. Mod. Phys. A. 2010. V. 25. P. 3505–3602;

   Kazakov D. I. Supersymmetry on the Run: LHC and Dark Matter // Nucl. Phys. Proc. Suppl. 2010. V. 203–204. P. 118–154;

   Ellis J. New Light on Dark Matter from the LHC. arXiv:1011.0077.

2. *Deshpande N. G., Ma E.* Pattern of Symmetry Breaking with Two Higgs Doublets // Phys. Rev. D. 1978. V. 18. P. 2574;

   Barbieri R., Hall L. J., Rychkov V. S. Improved Naturalness with a Heavy Higgs: An Alternative Road to LHC Physics // Phys. Rev. D. 2006. V. 74. P. 015007;

   Ginzburg I. F. et al. Evolution of Universe to the Present Inert Phase // Phys. Rev. D. 2010. V. 82. P. 123533.

3. *Lundstrom E., Gustafsson M., Edsjo J.* The Inert Doublet Model and LEP II Limits // Phys. Rev. D. 2009. V. 79. P. 035013.

4. *Dolle E. M., Su S.* The Inert Dark Matter // Ibid. V. 80. P. 055012;

   Dolle E. et al. Dilepton Signals in the Inert Doublet Model // Phys. Rev. D. 2010. V. 81. P. 035003;

   Lopez Honorez L. et al. The Inert Doublet Model: An Archetype for Dark Matter // JCAP. 2007. V. 0702. P. 028;

Nezri E., Tytgat M. H. G., Vertongen G. e^+ and Anti-p from Inert Doublet Model Dark Matter // JCAP. 2009. V. 0904. P. 014;

Andreas S., Hambye T., Tytgat M. H. G. WIMP Dark Matter, Higgs Exchange and DAMA // JCAP. 2008. V. 0810. P. 034;

Lopez Honorez L., Yaguna C. E. The Inert Doublet Model of Dark Matter Revisited // JHEP. 2010. V. 1009. P. 046;

5. *Kopylov G. I.* Just Kinematics. M.: Nauka, 1981;

Heuer R. D. et al. TESLA Technical Design Report. DESY 2001-011, TESLA Report 2001-23, TESLA FEL 2001-05. 2001;

Particle Data Group. The Review of Particle Physics // J. Phys. G. 2010. V. 37. P. 075021.